## Facilitating spin squeezing generated by collective dynamics with single-particle decoherence

K. Tucker, <sup>1,2</sup> D. Barberena, <sup>1,3</sup> R. J. Lewis-Swan, <sup>1,3</sup> J. K. Thompson, <sup>1</sup> J. G. Restrepo, <sup>2</sup> and A. M. Rey <sup>1</sup> JILA, NIST, Department of Physics, University of Colorado, Boulder, Colorado 80309, USA <sup>2</sup> Department of Applied Mathematics, University of Colorado, Boulder, Colorado 80309, USA <sup>3</sup> Center for Theory of Quantum Matter, University of Colorado, Boulder, Colorado 80309, USA



(Received 23 December 2019; accepted 7 October 2020; published 3 November 2020)

We study the generation of spin squeezing in arrays of long-lived dipoles subject to collective emission, coherent drive, elastic interactions, and single-particle relaxation. It is found that not only does single-particle relaxation not necessarily degrade the squeezing generated in the collective dynamics, but the interplay of single-particle and collective effects can in fact facilitate the generation of squeezing in a specific parameter regime. This latter behavior is connected to the dynamical self-tuning of the system through a dissipative phase transition that is present in the collective system alone. Our findings will be applicable to next-generation quantum sensors with an eye towards atomic clocks in cavity-QED setups and trapped ion systems.

DOI: 10.1103/PhysRevA.102.051701

Introduction. The preparation of entangled and nonclassical quantum states is a vital task for many quantum technologies, including metrology [1] and quantum information [2,3]. Conventional protocols generate entanglement via coherent dynamics and seek to minimize the decoherence induced by couplings to the environment [4,5]. However, it has been established that dissipation can itself be a powerful resource for entanglement generation under appropriate conditions. In particular, quantum reservoir engineering has established the potential to generate pure entangled steady states by carefully tailored couplings between the system and environment [6–12].

While these engineered dissipative systems can lead to rich physics, their realization is difficult. Ultracold atoms coupled to optical cavities and trapped ion arrays are emerging as a convenient platform where both coherent and dissipative dynamics can be engineered with great controllability [13–28]. In fact, these systems have garnered tremendous theoretical attention for many years [29-42] given the emergent new behaviors, critical phenomena, and quantum phases of matter that they can feature. For example, nonequilibrium phase transitions in collective models, featuring entangled steady states around critical points, have been identified as an appealing resource for quantum metrology [34,39-42]. However, a drawback is that the timescales required to reach the steady state are typically extremely long [30,34], specifically with respect to common experimental sources of technical noise and single-particle decoherence which are often neglected in the theoretical models. In view of this, the widely held expectation is that single-particle decoherence will strongly limit any entanglement generated by the collective dynamics.

Here, we demonstrate that the introduction of singleparticle decoherence in a collective driven-dissipative system, featuring a nonequilibrium phase transition, is not necessarily detrimental but instead can facilitate, under the restriction of fixed parameters, the generation of states with enhanced metrological utility relative to the steady state of the collective dynamics alone.

The mechanism driving this phenomenon is the destruction of collective coherence due to single-particle decoherence, which dynamically reduces the effective particle number, allowing the system to dynamically traverse the corresponding nonequilibrium phase diagram [see Fig. 1(a)], and in turn access regimes that may display large transient squeezing. While our analysis of this phenomenon is framed from a cavity-QED perspective, we note that similar conclusions can be drawn in more general models including arrays of trapped ions [24,25,39,43] and superconducting qubits [44,45].

*Model.* We consider an ensemble of N atoms in an optical lattice supported by a standing-wave optical cavity, illustrated in Fig. 1(b). A single common mode of the cavity couples two internal states of the atoms,  $|\uparrow\rangle$  and  $|\downarrow\rangle$ , which encode a spin-1/2 degree of freedom. To realize coherent driving of the dipoles the cavity is pumped with an external coherent field that is resonant with the atomic transition, and upon adiabatic elimination of the intracavity field [46] (which we assume evolves rapidly compared to relevant timescales) the dynamics of the atomic degrees of freedom can be described by a master equation for the atomic density operator  $\hat{\rho}$  [34],

$$\frac{\partial \hat{\rho}}{\partial t} = -\frac{i}{\hbar} [\hat{H}, \hat{\rho}] + L_c[\hat{\rho}] + L_s[\hat{\rho}], \tag{1}$$

$$\hat{H} = \hbar \chi \hat{J}_{+} \hat{J}_{-} + \hbar \Omega \hat{J}_{x}, \qquad (2)$$

where  $\hat{J}_{\alpha} = \sum_{i=1}^{N} \frac{1}{2} \hat{\sigma}_{i}^{\alpha}$  for  $\alpha = x, y, z, \hat{\sigma}_{i}^{\alpha}$  are the Pauli operators on the Hilbert space for each spin  $i=1,2,\ldots,N$ , and  $\hat{J}_{\pm} = \hat{J}_{x} \pm i\hat{J}_{y}$  are collective raising and lowering operators. The first term in  $\hat{H}$  corresponds to a collective exchange interaction realized by detuning the cavity from the atomic transition and characterized by  $\chi$ , and the second to a coherent drive characterized by  $\Omega$ . The dissipative part of Eq. (1) includes a collective decay term with rate  $\Gamma$  given by

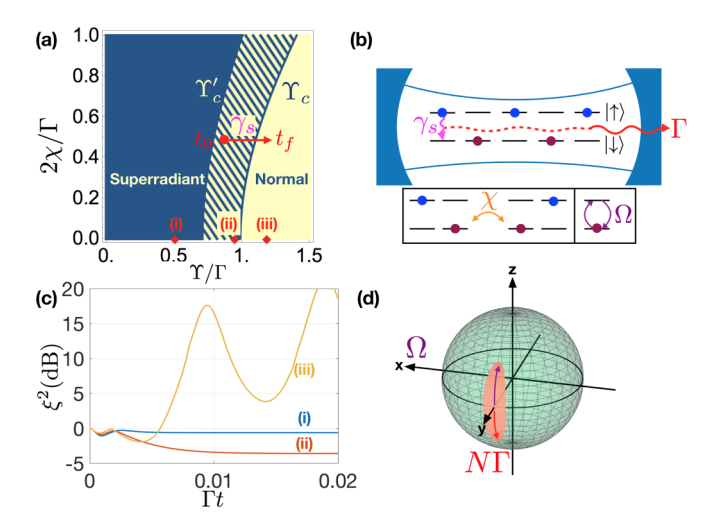


FIG. 1. (a) Steady-state phase diagram of an ensemble of N spin-1/2 particles subjected to a coherent drive with Rabi frequency  $\Omega = N\Upsilon/2$ , collective emission at rate  $\Gamma$ , collective spin-exchange interactions  $\chi$ , and single-particle relaxation at rate  $\gamma_s$ . This system can be engineered using an optical cavity (b) or trapped ion arrays. The spin-1/2 is encoded in a pair of electronic states, while the collective dissipation and global spin-spin interactions are mediated by spin-1/2's exchanging virtual bosons through a common mode. In the absence of single-particle relaxation, the system undergoes a nonequilibrium phase transition (superradiant to normal) signaled by a change in the total steady-state atomic inversion, which serves as an order parameter. Approaching the transition point from the superradiant phase [points (i) and (ii)], the coherent drive (in the  $\hat{x}$  direction) and collective emission combine to generate spin squeezing along  $\hat{x}$ , as shown in (c) and (d). In the normal phase no squeezing is observed [point (iii)]. For all three graphs in (c), N = 2000 and all spins are initially polarized along  $-\hat{x}$ . (d) explicitly displays the Bloch sphere overlaid with a squeezed collective spin distribution of the steady state (pink). Note that this is for illustrative purposes, and that the actual position and orientation of the squeezing can vary with parameters. Introducing finite  $\gamma_s$  allows the system to dynamically traverse the phase diagram [red arrow in (a)] and enhances the achievable spin squeezing in the striped region of (a).

 $L_c[\hat{\rho}] = \Gamma L(\hat{J}_-)[\hat{\rho}]$  arising due to leakage of the intracavity field via the mirrors. Both  $\chi$  and  $\Gamma$  are proportional to the single-particle cooperativity of the cavity [47]. We also include a single-particle relaxation channel with rate  $\gamma_s$  given by  $L_s[\hat{\rho}] = \gamma_s \sum_{i=1}^N L(\hat{\sigma}_i^-)[\hat{\rho}]$ , where the Lindblad superoperator is  $L(\hat{O})[\hat{\rho}] = \hat{O}\hat{\rho}\hat{O}^{\dagger} - \{\hat{O}^{\dagger}\hat{O}, \hat{\rho}\}/2$  for a given operator  $\hat{O}$ . This term accounts for the finite lifetime of the excited state of the transition induced from natural spontaneous emission or other systematic effects such as light scattering [48]. Other types of single-particle decoherence (e.g., dephasing) would result in similar behavior, though we only consider single-particle relaxation here.

Collective physics. Before discussing the effects of single-particle relaxation, we review the behavior of the collective system when  $\gamma_s = 0$ . As the dynamics is entirely described by collective operators, then the total spin operator  $\hat{J}^2 = \hat{J}_x^2 + \hat{J}_y^2 + \hat{J}_z^2$  is conserved during evolution. Consequently, if we restrict ourselves to initializing the atoms in a coherent spin state [49], which is an eigenstate of  $\hat{J}^2$  with

eigenvalue J(J+1) with J=N/2, then the available Hilbert space in which the dynamics and steady state exist is greatly reduced to only N+1 states (relative to  $2^N$  for N spin-1/2's). With this simplification, an analytic solution is available for the steady-state density operator  $\hat{\rho}_{ss}$  [30,34] from which all relevant collective spin observables can be computed. Previous work [30,34] has demonstrated that as a function of  $\Upsilon \equiv (2\Omega/N)$  and for large N, the steady state exhibits a nonequilibrium second-order phase transition in the thermodynamic limit, described by an abrupt change in behavior of the order parameter  $\langle \hat{J}_z \rangle$  at a critical value given by

$$\Upsilon_c = \sqrt{\Gamma^2 + 4\chi^2}.\tag{3}$$

The critical point separates a superradiant phase for  $\Upsilon < \Upsilon_c$  characterized by nonzero inversion  $|\langle \hat{J}_z \rangle| > 0$ , and a normal phase for  $\Upsilon > \Upsilon_c$  with zero inversion  $\langle \hat{J}_z \rangle = 0$  [see Fig. 1(a)]. The critical point  $\Upsilon_c$  also delineates regions in the phase diagram for which the steady state of the atomic ensemble is spin squeezed. The squeezing is characterized by the parameter [50]

$$\xi^{2} = \min_{\mathbf{n}_{\perp}} \frac{N(\Delta \hat{J}_{\mathbf{n}_{\perp}})^{2}}{\left|\langle \hat{\mathbf{J}} \rangle\right|^{2}},\tag{4}$$

where  $\langle \hat{\mathbf{J}} \rangle = (\langle \hat{J}_x \rangle, \langle \hat{J}_y \rangle, \langle \hat{J}_z \rangle)$  defines the collective Bloch vector,  $\mathbf{n}_{\perp}$  is a unit vector orthogonal to  $\langle \hat{\mathbf{J}} \rangle$ , and  $(\Delta \hat{J}_{\mathbf{n}_{\perp}})^2 = \langle (\hat{\mathbf{J}} \cdot \mathbf{n}_{\perp})^2 \rangle - \langle \hat{\mathbf{J}} \cdot \mathbf{n}_{\perp} \rangle^2$  is the variance of the collective spin operator in the direction of  $\mathbf{n}_{\perp}$ . Squeezing,  $\xi^2 < 1$ , is an entanglement witness and quantifies the utility of the spin state for quantum sensing applications [51].

Figure 1(c) illustrates that just below  $\Upsilon_c$  the steady state is squeezed, due to the finely balanced competition of the coherent drive and the nonlinear dynamics induced by the collective dissipation [see Fig. 1(d)]. Specifically, as  $\Upsilon$  approaches the threshold  $\Upsilon_c$  from below [curves (i) and (ii)], the system relaxes into an increasingly squeezed state with  $\xi^2 < 1$ . However, for  $\Upsilon > \Upsilon_c$  the squeezing is abruptly lost beyond an early transient. It should be noted that for  $\Upsilon < \Upsilon_c$  a careful selection of initial conditions becomes necessary to reach the squeezed steady state quickly, and to avoid an oscillatory phase known to exist near the critical point when  $|\chi| > 0$  [34]. It is also important to note that the squeezing is predominantly in the azimuthal direction for small  $\chi/\Gamma < 1$  [see Fig. 1(d) and Ref. [47]].

Effects of single-particle relaxation. When  $\gamma_s \neq 0$ , the collective  $\hat{J}^2$  symmetry is broken by the single-particle decoherence. This means the dynamics are free to explore a larger portion of the full Hilbert space of  $2^N$  states, compared to the limited N+1 states of the collective model. Due to this increased complexity, an analytic formula for the steady state is not available. However, a mean-field analysis can give useful insight into the steady-state phase diagram of the system, including the position of critical transitions and transient behavior. These predictions can be confirmed by efficient numerical simulation [52–54] of the full quantum dynamics described by the master equation [Eq. (1)], which also allows us to investigate quantum features such as spin squeezing. In the mean-field approximation, we generate equations of motion for the expectation values  $\langle \hat{\sigma}_i^{\alpha}(t) \rangle$  (identical for

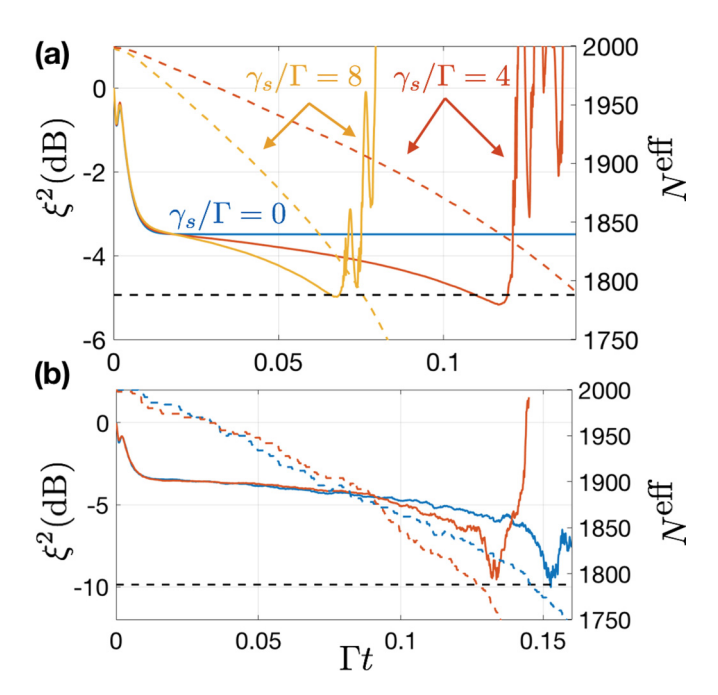


FIG. 2. (a) Squeezing vs time for N=2000,  $\chi/\Gamma=0$ ,  $\Upsilon/\Upsilon_c=0.9$ , and a range of  $\gamma_s/\Gamma$ . Solid lines indicate squeezing  $\xi^2(t)$  and dashed lines the corresponding time-dependent effective system size  $N^{\rm eff}(t)$  (matching colors). The horizontal black line corresponds to the critical effective particle number  $N_c=2\Omega/\Upsilon_c$  for which the transition between superradiant and normal phases occurs. (b) Squeezing  $\xi^2(t)$  (solid) and effective system size  $N^{\rm eff}(t)$  (dashed) computed from two individual trajectories of the numerical method with  $\gamma_s/\Gamma=4$ . For each trajectory,  $N^{\rm eff}(t)$  crosses the horizontal line for  $N_c$  near the point where its corresponding  $\xi^2(t)$  reaches a minimum. In each panel, all spins are initially polarized along  $-\hat{x}$ .

all particles due to permutational symmetry) from Eq. (1) and assume that all higher-order expectations factorize, i.e.,  $\langle \hat{\sigma}_{i}^{\alpha}(t) \hat{\sigma}_{j}^{\beta}(t) \rangle = \langle \hat{\sigma}_{i}^{\alpha}(t) \rangle \langle \hat{\sigma}_{j}^{\beta}(t) \rangle$  for  $i \neq j$  [47].

The mean-field analysis indicates that many of the qualitative features of the collective physics, particularly the steady-state behavior, remain when single-particle relaxation is included. Specifically, for  $\gamma_s \neq 0$  there is a critical point  $\Upsilon'_c \equiv \Upsilon_c/\sqrt{2}$  delineating superradiant and normal phases characterized by the long-time limit of collective observables. Moreover, numerical simulations of the full quantum dynamics reveal that  $\Upsilon'_c$  also marks the boundary between a squeezed steady state in the superradiant phase and the absence of long-time squeezing in the normal phase [47]. This transition is illustrated in Fig. 1(a).

Impact on squeezing. We now turn our focus to a quantitative analysis of the effects of decoherence on the achievable spin squeezing, both in the steady state and in the transient dynamics. Naively, one might expect that single-particle relaxation only leads to a degradation of the squeezing generated by the collective dynamics [55]. Between  $\Upsilon'_c < \Upsilon < \Upsilon_c$  [striped region (ii), Fig. 1(a)] we find appreciable squeezing develops in the transient dynamics on a timescale for which both collective and single-particle effects are relevant. In particular, the predicted squeezing exceeds what is seen in the collective steady state for  $\gamma_s = 0$ .

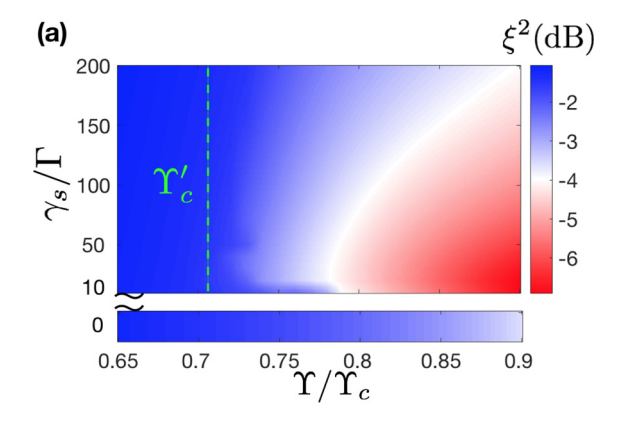
Figure 2(a) illustrates the spin-squeezing dynamics in this region  $\Upsilon_c' < \Upsilon < \Upsilon_c$  for several values of  $\gamma_s/\Gamma$  and in the absence of elastic interactions ( $\chi/\Gamma=0$ ). We observe that, as expected, squeezing does not persist in a steady state as it does in the purely collective case ( $\gamma_s/\Gamma=0$ ). However, we see that squeezing still develops and persists at timescales  $\sim 1/\gamma_s$ , and that it exceeds the purely collective steady-state squeezing for  $\chi=0$  and the same values of  $\Upsilon/\Upsilon_c$ . The results of the figure indicate that the achievable spin squeezing remains relatively robust to the precise value of  $\gamma_s/\Gamma$ . Instead, the magnitude of  $\gamma_s$  effectively only controls the timescales over which the enhanced squeezing is obtained (i.e., it controls the rate at which we dynamically traverse the related collective steady-state phase diagram—which ultimately sets the bound on the achievable squeezing).

Squeezing mechanism. The transient squeezing for  $\Upsilon_c' < \Upsilon < \Upsilon_c$  occurring at timescales  $\sim 1/\gamma_s$  can be understood within the framework of the collective steady state. Specifically, the enhancement can be understood as a subtle consequence of the destruction of collective coherence by single-particle dissipation. We argue that reducing the collective coherence leads to an effective increase of  $\Upsilon$  over time  $[\Upsilon \to \Upsilon^{\rm eff}(t)]$ , which allows the system to dynamically traverse the collective phase diagram into regions with higher spin squeezing.

Our argument is illustrated by plotting in Fig. 2(a) the time evolution of an effective atom number related to the total spin  $\hat{J}^2$  as  $N^{\rm eff}(t) \equiv 2\sqrt{(1/4) + \langle \hat{J}^2 \rangle(t)} - 1$ . For  $\gamma_s = 0$  we have  $N^{\rm eff}(t) = N$ , but for  $\gamma_s > 0$  we observe the effective system size decays,  $N^{\rm eff}(t) \leq N$ , making  $\Upsilon^{\rm eff}(t) \equiv 2\Omega/N^{\rm eff}(t)$  grow over time even though the coherent drive remains constant.

One can therefore dynamically approach and even cross the critical point  $\Upsilon_c$  as the system evolves. This is confirmed by the strong correlation between the timing of the crossing of the threshold atom number,  $N^{\rm eff}(t^*)$  [determined from  $\Upsilon^{\rm eff}(t^*) = \Upsilon_c$  and indicated by a dashed horizontal line in Fig. 2] and the loss of squeezing for  $t > t^*$  for the different  $\gamma_s$ . This provides evidence that squeezing is dynamically lost as the system effectively transitions from the superradiant to normal phases, corresponding to the crossover from squeezed to unsqueezed regimes in the collective model.

However, in Fig. 2(a), we observe a small quantitative disagreement between these timescales. To confirm the idea that squeezing disappears as a result of  $\Upsilon^{\text{eff}}$  crossing to the normal phase and demonstrate that the observed deviation in the averaged quantities is a result of quantum noise, in Fig. 2(b) we perform an investigation of individual trajectories, which mimic a typical experimental realization. We use these trajectories to simulate the open system dynamics via a Monte Carlo wave-function method which unravels the evolution of the density matrix [Eq. (1)] into an ensemble of pure state wave functions evolving accordingly to a non-Hermitian Hamiltonian. Dissipation is further incorporated within each of these independent trajectories by stochastic jumps that project the wave function [47]. As shown in Fig. 2(b), in a single trajectory squeezing features an abrupt change in behavior exactly for  $t > t^*$ . However, as visible in Fig. 2, the fact that  $t^*$  varies from trajectory to trajectory explains, on the one hand, the moderate discrepancy in timescales mentioned



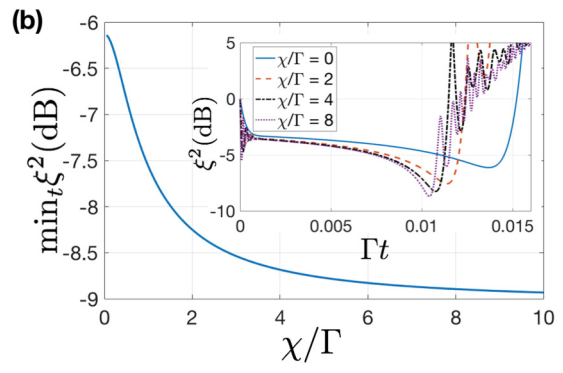


FIG. 3. (a) Minimum transient spin squeezing (see text for clarification) as a function of normalized drive amplitude  $\Upsilon/\Upsilon_c$  and relaxation rate  $\gamma_s/\Gamma$  with  $\chi/\Gamma=0$ . The strip below the main panel shows a magnified view of the  $\gamma_s/\Gamma=0$  result for comparison. Note the break in the vertical axis, which is required since attainable simulation times cannot capture the squeezing behavior occurring on timescales of  $1/\gamma_s$  when this value is very large. (b) Minimum transient spin squeezing as a function of the interaction strength  $\chi/\Gamma$ with fixed  $\Upsilon/\Upsilon_c = 0.9$  and  $\gamma_s/\Gamma = 50$ . Inset: Squeezing vs time for a selection of values of  $\chi/\Gamma$  and the same  $\Upsilon$ ,  $\gamma_s$  as the main panel. For (a) and (b) we compute the dynamics using a truncated cumulant expansion [47] and  $N = 10^4$ . Initial conditions in (a) are the coherent spin state (CSS) in the  $-\hat{x}$  direction, and in (b) are taken to be the CSS in the direction of the mean-field steady state (for each  $\chi/\Gamma$ and  $\Upsilon$ ) when  $\gamma_s/\Gamma=0$  to account for the rotations that result from different values of  $\chi/\Gamma$ .

above and, on the other, the net reduction on the optimal observed squeezing when an average over many trajectories is taken. The latter is necessary to recover the master equation results. Related to this last point, we note that these results indicate that sources of technical noise, such as shot-to-shot fluctuations in the atom number will need to be kept sufficiently small (i.e., sub-Poissonian) as they can also lead to a smearing out of the crossover into the superradiant phase and reduce the achievable squeezing overall.

In Fig. 3(a) we investigate the minimum squeezing obtained in the transient dynamics, after the initial collective minimum, as a function of the normalized drive amplitude  $\Upsilon$  and single-particle relaxation rate  $\gamma_s/\Gamma$ . The introduction of finite  $\gamma_s/\Gamma \neq 0$  clearly improves the attainable squeezing within the region of  $\Upsilon'_c < \Upsilon < \Upsilon_c$  relative to the collective case  $(\gamma_s/\Gamma = 0$ , shown in the lower strip). This improvement occurs for even relatively small values of  $\gamma_s$ , although as

 $\gamma_s$  is increased the best transient squeezing, attained for  $\Upsilon$  approaching  $\Upsilon_c$ , gradually degrades. On the other hand, for  $\Upsilon < \Upsilon_c'$  a stable steady state is quickly reached and squeezing is not enhanced by introducing single-particle decoherence.

While our qualitative understanding of the mechanism driving squeezing has so far not included a discussion of the collective exchange interactions, the achievable squeezing does quantitatively depend on  $\chi$  for  $\Upsilon < \Upsilon'_c$ . This is demonstrated in Fig. 3(b), where we plot the minimum transient squeezing as a function of  $\chi/\Gamma$  for  $\gamma_s/\Gamma = 50$ . It is apparent that increasing the interaction strength  $\chi$  leads to an appreciable improvement in the optimal squeezing, particularly in the region  $0 < \chi/\Gamma \lesssim 2$ . However, the inset of Fig. 3(b) indicates that an increased interaction strength does not significantly change the qualitative dynamics of the squeezing, beyond the generation of an earlier transient (absent in the  $\chi = 0$ case). This earlier transient that appears at finite  $\chi$  might be useful for some platforms, but on the other hand for purely metrological applications might be not as practical in cases such as the cavity setup discussed below [47]. There, although feasible, technical challenges come up when quenching  $\chi$ sufficiently fast to take advantage of the earlier transient squeezing.

Experimental realization and outlook. The spin model we have discussed could be realized by coupling an optical cavity to the narrow linewidth optical clock transitions available in alkaline-earth atoms [14,15]. We require that  $\kappa \gg g\sqrt{N}$  and  $\kappa \gg \gamma_s$  (bad cavity limit) with 2g the single-photon Rabi frequency and  $\kappa$  the cavity linewidth, to ensure that the intracavity field can be adiabatically eliminated and thus realize the desired spin model [Eqs. (1) and (2)]. In this limit, spinspin interactions can be engineered by detuning the cavity from the atomic transition by  $\Delta_c$  which leads to a tunable interaction strength  $\chi = 4g^2\Delta_c/(4\Delta_c^2 + \kappa^2)$ . Similarly, the collective dissipation arises due to photon leakage and is characterized by  $\Gamma = 4g^2\kappa/(4\Delta_c^2 + \kappa^2)$  [14,56]. To ensure that decoherence is not too large such that it eliminates any possibility of squeezing, we need to operate in the limit of a large (effective) collective cooperativity  $\gamma_s \lesssim N\Gamma$ . This condition, together with those for  $\kappa$  above, imply we should work in the hierarchy of energy scales  $\gamma_s \lesssim N\Gamma \ll g\sqrt{N} \ll \kappa$  to generate spin squeezing in the cavity platform. The possibility to operate in this regime has previously been demonstrated using both the  ${}^{1}S_{0}$  -  ${}^{3}P_{0}$  transition in  ${}^{87}Sr$  [14,56] and  ${}^{1}S_{0}$  -  ${}^{3}P_{1}$ transition in <sup>88</sup>Sr [15]. The former has a natural linewidth of  $\gamma \approx 2\pi \times 1$  mHz and  $2g = 2\pi \times 8$  Hz [14]. State-of-theart atomic, molecular, and optical (AMO) experiments have demonstrated a coherence of the  ${}^{1}S_{0}$  -  ${}^{3}P_{0}$  transition of up to  $1/\gamma_s \approx 10$  s [48] which corresponds to  $\gamma_s/\Gamma \approx 200$  for  $\Delta_c = \kappa = 2\pi \times 150$  kHz and thus  $\chi/\Gamma \approx 1$ . For  $N \sim 10^4$ atoms, dissipatively enhanced squeezing of  $\xi^2 \approx 9$  dB is then in principle achievable on timescales  $t \sim 2$  s.

A similar implementation can also be realized in trapped ion arrays, where a pseudospin-1/2 is encoded in the hyperfine states of the ion. As carefully shown in Ref. [43], it is possible to engineer in a Penning trap the same collective dissipation that is responsible for superradiance in cavity-QED systems. This is achieved by loading two types of ions ( $\tau$  and  $\sigma$ ) into a shared trap. The two species could be, for example, two different elements, or isotopes of the same element. The

 $\tau$  ions are used to sympathetically cool the normal modes of vibration of the system of ions and generate an effective phonon loss, analogous to  $\kappa$  in the cavity platform. Further, by Doppler cooling the  $\tau$  ions it is possible to introduce couplings between the normal modes, resulting in a new dressed set of damped normal modes. The  $\sigma$  ions then serve as the effective spins that are squeezed through interactions mediated by the damped phonon modes. The  $\sigma$  ion-phonon coupling can be engineered using an optical dipole force generated via pairs of Raman beams. The detuning of the Raman beams can be set such that predominantly the center-of-mass (c.m.) mode is excited (i.e., the other mode remains off resonant), such that the c.m. mode plays the role of the common cavity mode which mediates both elastic [24] and inelastic collective spin interactions between the ions. Additionally, resonant microwaves can be used to coherently directly drive the spins [25]. As analyzed in detail in Ref. [43], using  $^{24}$ Mg<sup>+</sup> ions as the  $\tau$  ions and  $^{25}\text{Mg}^+$  as the  $\sigma$  ions, it should be possible to achieve an effective  $\Gamma \sim 2\pi \times \text{Hz}$  in a system of the order of N=124 $\sigma$  ions. In this implementation the average single-particle decoherence generated by the Raman beams including effective

spontaneous emission, absorption, and dephasing is of the order of  $\bar{\gamma}_s \sim 2\pi \times \text{Hz}$ . In this setup therefore it should be possible to operate in the regime where  $N\Gamma/\bar{\gamma}_s \sim 100$  and reach the conditions required for robust spin-squeezing generation.

In summary, we have identified an intriguing and experimentally relevant situation where spin squeezing can coexist with relatively large single-particle decoherence as long as collective decoherence remains the dominant dissipative process. We expect our results to have immediate applications for quantum metrology, specifically in the generation of squeezing on long-lived optical transitions for next-generation optical atomic clocks, while also being relevant for quantum simulation.

Acknowledgments. We are grateful for feedback from M. A. Norcia and J. T. Young on the manuscript. This work is supported by the AFOSR Grant No. FA9550-18-1-0319, by the DARPA and ARO Grant No. W911NF-16-1-0576, the ARO single investigator Award No. W911NF-19-1-0210, the NSF Grant No. PHY1820885, NSF JILA-PFC PHY-1734006 grants, and by NIST.

- L. Pezzè, A. Smerzi, M. K. Oberthaler, R. Schmied, and P. Treutlein, Rev. Mod. Phys. 90, 035005 (2018).
- [2] *The Physics of Quantum Information*, edited by D. Bouwmeester, A. Ekert, and A. Zeilinger (Springer, Berlin, 2000).
- [3] S. Braunstein and A. Pati, *Quantum Information with Continuous Variables* (Springer, Dordrecht, 2012).
- [4] R. J. Lewis-Swan, M. A. Norcia, J. R. K. Cline, J. K. Thompson, and A. M. Rey, Phys. Rev. Lett. 121, 070403 (2018).
- [5] J. Hu, W. Chen, Z. Vendeiro, A. Urvoy, B. Braverman, and V. Vuletić, Phys. Rev. A 96, 050301(R) (2017).
- [6] B. Kraus, H. P. Büchler, S. Diehl, A. Kantian, A. Micheli, and P. Zoller, Phys. Rev. A 78, 042307 (2008).
- [7] S. Diehl, A. Micheli, A. Kantian, B. Kraus, H. P. Büchler, and P. Zoller, Nat. Phys. 4, 878 (2008).
- [8] E. G. Dalla Torre, J. Otterbach, E. Demler, V. Vuletic, and M. D. Lukin, Phys. Rev. Lett. 110, 120402 (2013).
- [9] M. J. Kastoryano, F. Reiter, and A. S. Sørensen, Phys. Rev. Lett. 106, 090502 (2011).
- [10] H. Krauter, C. A. Muschik, K. Jensen, W. Wasilewski, J. M. Petersen, J. I. Cirac, and E. S. Polzik, Phys. Rev. Lett. 107, 080503 (2011).
- [11] Y. Lin, J. P. Gaebler, F. Reiter, T. R. Tan, R. Bowler, A. S. Sørensen, D. Leibfried, and D. J. Wineland, Nature (London) 504, 415 (2013).
- [12] J. F. Poyatos, J. I. Cirac, and P. Zoller, Phys. Rev. Lett. 77, 4728 (1996).
- [13] B. Braverman, A. Kawasaki, E. Pedrozo-Peñafiel, S. Colombo, C. Shu, Z. Li, E. Mendez, M. Yamoah, L. Salvi, D. Akamatsu, Y. Xiao, and V. Vuletić, Phys. Rev. Lett. 122, 223203 (2019)
- [14] M. A. Norcia, R. J. Lewis-Swan, J. R. K. Cline, B. Zhu, A. M. Rey, and J. K. Thompson, Science 361, 259 (2018).
- [15] J. A. Muniz, D. Barberena, R. J. Lewis-Swan, D. J. Young, J. R. K. Cline, A. M. Rey, and J. K. Thompson, Nature 580, 602 (2020).

- [16] I. D. Leroux, M. H. Schleier-Smith, and V. Vuletić, Phys. Rev. Lett. 104, 073602 (2010).
- [17] E. J. Davis, G. Bentsen, L. Homeier, T. Li, and M. H. Schleier-Smith, Phys. Rev. Lett. 122, 010405 (2019).
- [18] V. D. Vaidya, Y. Guo, R. M. Kroeze, K. E. Ballantine, A. J. Kollár, J. Keeling, and B. L. Lev, Phys. Rev. X 8, 011002 (2018).
- [19] O. Hosten, R. Krishnakumar, N. J. Engelsen, and M. A. Kasevich, Science 352, 1552 (2016).
- [20] M. P. Baden, K. J. Arnold, A. L. Grimsmo, S. Parkins, and M. D. Barrett, Phys. Rev. Lett. 113, 020408 (2014).
- [21] J. Kohler, N. Spethmann, S. Schreppler, and D. M. Stamper-Kurn, Phys. Rev. Lett. 118, 063604 (2017).
- [22] K. Baumann, C. Guerlin, F. Brennecke, and T. Esslinger, Nature (London) **464**, 1301 (2010).
- [23] F. Brennecke, T. Donner, S. Ritter, T. Bourdel, M. Köhl, and T. Esslinger, Nature (London) **450**, 268 (2007).
- [24] J. G. Bohnet, B. C. Sawyer, J. W. Britton, M. L. Wall, A. M. Rey, M. Foss-Feig, and J. J. Bollinger, Science 352, 1297 (2016).
- [25] A. Safavi-Naini, R. J. Lewis-Swan, J. G. Bohnet, M. Gärttner, K. A. Gilmore, J. E. Jordan, J. Cohn, J. K. Freericks, A. M. Rey, and J. J. Bollinger, Phys. Rev. Lett. 121, 040503 (2018).
- [26] J. Zhang, G. Pagano, P. W. Hess, A. Kyprianidis, P. Becker, H. Kaplan, A. V. Gorshkov, Z.-X. Gong, and C. Monroe, Nature (London) 551, 601 (2017).
- [27] P. Jurcevic, H. Shen, P. Hauke, C. Maier, T. Brydges, C. Hempel, B. P. Lanyon, M. Heyl, R. Blatt, and C. F. Roos, Phys. Rev. Lett. 119, 080501 (2017).
- [28] J. T. Barreiro, M. Müller, P. Schindler, D. Nigg, T. Monz, M. Chwalla, M. Hennrich, C. F. Roos, P. Zoller, and R. Blatt, Nature (London) 470, 486 (2011).
- [29] D. F. Walls, P. D. Drummond, S. S. Hassan, and H. J. Carmichael, Prog. Theor. Phys. Suppl. 64, 307 (1978).
- [30] H. J. Carmichael, J. Phys. B: At. Mol. Phys. 13, 3551 (1980).
- [31] P. D. Drummond, Phys. Rev. A 22, 1179 (1980).

- [32] P. D. Drummond and S. S. Hassan, Phys. Rev. A 22, 662 (1980).
- [33] P. D. Drummond and H. J. Carmichael, Opt. Commun. 27 (1978).
- [34] D. Barberena, R. J. Lewis-Swan, J. K. Thompson, and A. M. Rey, Phys. Rev. A 99, 053411 (2019).
- [35] S. Morrison and A. S. Parkins, J. Phys. B: At., Mol. Opt. Phys. 41, 195502 (2008).
- [36] J. Li and G. S. Paraoanu, New J. Phys. 11, 113020 (2009).
- [37] T. E. Lee, F. Reiter, and N. Moiseyev, Phys. Rev. Lett. 113, 250401 (2014).
- [38] T. E. Lee and C.-K. Chan, Phys. Rev. A 88, 063811 (2013).
- [39] S. Schneider and G. J. Milburn, Phys. Rev. A 65, 042107 (2002).
- [40] A. González-Tudela and D. Porras, Phys. Rev. Lett. 110, 080502 (2013).
- [41] T. E. Lee, C.-K. Chan, and S. F. Yelin, Phys. Rev. A 90, 052109 (2014).
- [42] E. Wolfe and S. F. Yelin, arXiv:1405.5288.
- [43] A. Shankar, J. Cooper, J. G. Bohnet, J. J. Bollinger, and M. Holland, Phys. Rev. A 95, 033423 (2017).
- [44] J. M. Fink, R. Bianchetti, M. Baur, M. Göppl, L. Steffen, S. Filipp, P. J. Leek, A. Blais, and A. Wallraff, Phys. Rev. Lett. 103, 083601 (2009).

- [45] J. A. Mlynek, A. A. Abdumalikov, C. Eichler, and A. Wallraff, Nat. Commun. 5, 5186 (2014).
- [46] R. Bonifacio, P. Schwendimann, and F. Haake, Phys. Rev. A 4, 302 (1971).
- [47] See Supplemental Material at http://link.aps.org/supplemental/ 10.1103/PhysRevA.102.051701 for details of simulation methods and experimental implementation.
- [48] R. B. Hutson, A. Goban, G. E. Marti, L. Sonderhouse, C. Sanner, and J. Ye, Phys. Rev. Lett. 123, 123401 (2019).
- [49] J. M. Radcliffe, J. Phys. A: Gen. Phys. 4, 313 (1971).
- [50] D. J. Wineland, J. J. Bollinger, W. M. Itano, F. L. Moore, and D. J. Heinzen, Phys. Rev. A 46, R6797(R) (1992).
- [51] M. Kitagawa and M. Ueda, Phys. Rev. A 47, 5138 (1993).
- [52] Y. Zhang, Y. Zhang, and K. Molmer, New J. Phys. 20, 112001 (2018).
- [53] K. Mølmer, Y. Castin, and J. Dalibard, J. Opt. Soc. Am. B 10, 524 (1993).
- [54] M. B. Plenio and P. L. Knight, Rev. Mod. Phys. 70, 101 (1998).
- [55] N. Shammah, S. Ahmed, N. Lambert, S. De Liberato, and F. Nori, Phys. Rev. A 98, 063815 (2018).
- [56] M. A. Norcia, M. N. Winchester, J. R. K. Cline, and J. K. Thompson, Sci. Adv. 2, e1601231 (2016).